LASER APPLICATIONS AND OTHER TOPICS IN QUANTUM ELECTRONICS

PACS numbers: 42.62.Fi; 78.47.+p; 78.20.-e; 78.20.Bh
DOI: 10.1070/QE2000v030n02ABEH001682

Nonlinear response of ultrathin Ni films in degenerate four-photon spectroscopy

L P Kuznetsova, V M Petnikova, K V Rudenko, V V Shuvalov

Abstract. The ultrathin (17 – 25 nm thick) continuous Ni films deposited on K8 glass and ZrO_2 substrates are experimentally studied. The degenerate four-photon spectroscopy showed typical resonances in the dependence of the self-diffraction efficiency on the wavelength of pump components. It is shown within the framework of the model of electronic cubic nonlinear susceptibility — taking into account the real structure of the spectrum of electronic states of Ni, its quantum-size renormalisation and spin splitting, the inter- and intraband relaxation, saturation, and the selection rules for the electronic transitions — that the electronic subsystem makes the dominant contribution to the nonlinear response of Ni films to picosecond laser pulses (20 ps long) in the 620 – 634 nm spectral range. The interband-polarisation relaxation time T_2 was found to be $\sim$200 fs.

1. Introduction

Recently, interest in the study of physical properties of ultrathin metallic films has increased [1 – 3]. This is mainly related to the demands of rapidly developing micro- and nanoelectronics. However, these studies are of considerable scientific interest as well. The point is that because the concentration of free carriers in metals is high (10^{21} – 10^{23} cm^{-3}), the electron – electron scattering at the subpicosecond scale should be the dominant mechanism of scattering in metals [1, 2]. In addition, one can observe the so-called quantum-size effect in ultrathin films [3, 4], which is absent in bulk samples. Knowledge of the real spectra of electronic states and kinetics of relaxation processes is required to understand many fundamental and technological properties of metals. Recently, a number of papers devoted to the study of the kinetics of ultrafast processes in ultrathin metal (including ferromagnetic) films by optical methods have been published. The probing of transmittance and/or reflectivity of a sample preliminarily excited by a femtosecond laser pulse [2], photoemission spectroscopy [1], and some other methods have been used.

In Ref. [5], ultrathin Ni films (with thickness $L = 17 - 25$ nm) were experimentally studied by using picosecond biharmonic pumping (BP). Typical side resonances observed in the wing of the dependence of the self-diffraction efficiency η on the frequency detuning Δ of biharmonic pump components were interpreted within the framework of the model of electronic cubic nonlinear susceptibility described in that paper. The model takes into account the real structure of the spectrum of electronic states of Ni, its quantum-size renormalisation and spin splitting, inter- and intraband relaxation, the selection rules for the electronic transitions, the saturation of the latter, etc. For the interband-polarisation relaxation times $T_2 > 200$ fs, the calculated dependences were in qualitative agreement with the experimental data. The results obtained show that, in the frequency degenerate case, which corresponds to the degenerate four-photon spectroscopy (DFPS) method, the electronic part of the nonlinear response should sharply decrease in the vicinity of certain points on the frequency scale.

The aim of our work was to verify experimentally this last statement, i.e., to carry out an experimental study of the efficiency of the nonlinear response of ultrathin Ni films as a function of the wavelength λ of pump components in the DFPS method and to interpret the experimental data on the basis of the model [5]. The task was to obtain a qualitative agreement between the calculated and the experimental dependences $\eta(\lambda)$ by varying the free parameters of the model and to obtain the desired spectroscopic information in this way.

2. DFPS method

In nonlinear spectroscopy of condensed media, methods based on two-photon excitation and probing of the electronic transitions [6], which are referred to as four-photon spectroscopy methods, are well known. It is reasonable to subdivide them into dynamic (nonstationary) and stationary methods. The light pulses used in stationary spectroscopy are considerably longer than the time scale of the processes under study. In this case, two picosecond laser pulses with frequencies $\omega_{1,2}$ and wave vectors $\boldsymbol{k}_{1,2}$, which travel at a certain angle to each other, interfere in the medium being studied and excite inside it a 'packet' of electronic excitations at the difference frequency $\Delta = \omega_1 - \omega_2$. An excited electron interacts with a thermostat and imparts to it the electron momentum 'defect' $\delta\boldsymbol{K} = \boldsymbol{k}_1 - \boldsymbol{k}_2$. A thermostat may represent acoustic and optical phonons, other electrons and holes, surface excitations, the so-called spin waves, etc.

Simultaneously with pumping, the excited medium is probed with a beam, which may have the same frequency $\omega_3 = \omega_1$ and the same wave vector $\boldsymbol{k}_3 = \boldsymbol{k}_1$ as one of the pump components. The probe beam is diffracted by low-frequency excitations of the medium (self-diffraction) resulting in the formation of the polarisation wave and the light field at the combination frequency $\omega_4 = \omega_3 + \omega_1 - \omega_2$ with the wave

L P Kuznetsova, V M Petnikova, K V Rudenko, V V Shuvalov
M V Lomonosov Moscow State University, Vorobyevy gory, 119899 Moscow, Russia

Received 13 September 1999
Kvantovaya Electronika **30** (2) 175 – 179 (2000)
Translated by A N Kirkin, Edited by M N Sapozhnikov

vector $\boldsymbol{k}_4 = \boldsymbol{k}_3 + \boldsymbol{k}_1 - \boldsymbol{k}_2$. In the DFPS method [7] that was used in the experiments described below, the detected signal coincided in frequency with the pump waves ($\omega_4 = \omega_{1,2,3}$) but propagated in a different direction: $\boldsymbol{k}_4 = 2\boldsymbol{k}_1 - \boldsymbol{k}_2; \boldsymbol{k}_1 = \boldsymbol{k}_3 \neq \boldsymbol{k}_2$. In the experiment, we measured the dependence of the efficiency η of the nonlinear process on the frequency $\omega_4 = \omega_{1,2,3}$ (the wavelength $\lambda_4 = \lambda_{1,2,3}$) of the pump components. The DFPS method allows one to identify and qualitatively determine positions, widths, and relations between amplitudes of the spectral features related to different physical processes contributing to the nonlinear response [7].

Note that each experimental point on the dependence $\eta(\lambda)$ in the DFPS method simultaneously represents an initial point ($\Delta = 0$) for the corresponding experimental dependence $\eta(\Delta)$ in the BP method. As will be seen below, this fact is very important for a combined analysis of the experimental data obtained by the two above methods of stationary four-photon spectroscopy.

3. Experiment

The experiment was carried out on the setup described in Ref. [5]. The pulses produced by two independently tunable picosecond dye lasers (20 ps long, with peak power up to 50 kW and spectral width of 1.5 cm^{-1}) were synchronised, focused, and directed at an angle of 7 ° into a sample. To tune the experimental setup to the point corresponding to the coincidence of dye laser pulses in frequency, time, and space, we used the correlation technique, i.e., the maximum efficiencies of noncollinear SHG in a KDP crystal ($L = 1$ mm) and self-diffraction both in thin ($L = 10 - 20$ μm) monocrystalline GaSe semiconductor films and directly in the Ni films under study.

At each experimental point, we made a series of measurements in which the oscillation wavelength of one dye laser ($\lambda = \lambda_1$) was fixed, whereas the wavelength of the other dye laser ($\lambda = \lambda_2$) was varied in order to tune the system to the maximum efficiency of the nonlinear process ($\lambda_2 = \lambda_1$). The wavelengths of pump components $\lambda_{1,2}$ were varied in the 620 – 634 nm range, their polarisations were parallel to one another and the film surface, and the initial temperature of samples was 300 K. The sensitivity in the channel of self-diffraction signal detection reached 10^{-16} J $pulse^{-1}$.

The output signals of photodetectors were processed by a computer, which carried out preliminary statistical processing of data and rejected the realisations that fell outside the 'gate' specified by the computer in the domain of parameters of the four signals being detected. This provided a considerable decrease (down to 10%) in the standard deviation of the desired signal.

The samples used in the experiments represented continuous ultrathin ($L = 17 - 25$ nm) Ni films deposited by laser evaporation onto K8 glass and ZrO_2 substrates. Mechanical and chemical polishing of the working faces of the substrates ensured that their roughness was as small as 5 nm. Prior to evaporation we selected the polished substrates characterised by minimum scattering. The film thickness was controlled both directly during the evaporation (by the number of laser pulses) and after the film preparation (with the aid of x-ray reflectometry).

Fig. 1 presents the results of measurements of the dependence of the self-diffraction efficiency η on the pump wavelength λ for a Ni film with thickness $L = 17$ nm. Using the least-squares method, the solid line was calculated by the

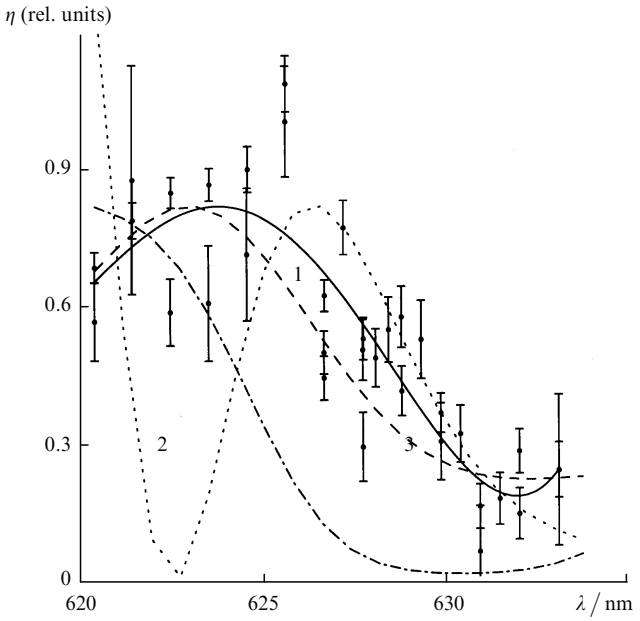

Figure 1. Experimental dependences of the nonlinear response η on the pump wavelength λ (points) and their approximation (solid curve) for the Ni film with thickness $L = 17$ nm, and the results of the calculation for the ferromagnetic [with (1) and without (2) allowance for the spin selection rules] and paramagnetic (3) phases for $L = 5$ nm, $\Theta_e = 600$ K, $s = 0.01$, and $T_2 = 200$ fs.

polynomial approximation of the experimental data (the mean-square deviation by one point corresponds to the experimental error). One can clearly see two typical spectral features. The efficiency of the process has a maximum at $\lambda \sim 624$ nm and a minimum at $\lambda \sim 632$ nm.

Note that the results of three series of measurements (with different positions of the focal point in the sample) are in agreement. This suggests that either the samples used by us were virtually homogeneous or the inhomogeneities were much smaller in size than the focal region (100 – 150 μm) of the dye laser beam. Note that the presence of a dip at $\lambda \sim 632$ nm in the electronic part of the nonlinear response Ni was predicted in Ref. [5] and agrees with the data of the experiments conducted in Refs [8 – 10] on nonlinear spectroscopy of YBaCuO, Cu, and C_{60} films, which were based on a similar idea.

4. Results of the numerical calculation

To interpret the experimental results we used the model described in Ref. [5]. Recall that this model is characterised by a certain freedom in the choice of a number of fitting parameters, such as the interband-polarisation relaxation time T_2, the temperature Θ_e of the electronic subsystem, the degree of maximum saturation (relative change in the occupation numbers) for electronic transitions s, etc. The numerical simulation in which we varied precisely these parameters and used the agreement between the calculated dependences and the experimental data as a criterion formed the basis of the procedure for obtaining the desired spectroscopic data.

In practice, this procedure was as follows. Numerical simulations gave us a series of dependences $\eta(\Delta)$ calculated for the nonlinear response of ultrathin Ni films for different values of free parameters (see above), including the presence or

lifting of selection rules for transitions between different subbands. The values of free parameters were regarded as allowable only in the cases where the dependences $\eta(\Delta)$ calculated for the BP method contained resonant features ('dips') in a range of frequency detunings of $\sim 150-200$ cm^{-1}, which were described in Ref. [5], and the spectral positions of specific features (the regions corresponding to the maximum and minimum self-diffraction efficiencies) in the dependences $\eta(\lambda)$ calculated for the DFPS method and the dynamic range of variation of $\eta(\lambda)$ (the relation between the maximum and minimum values of η in the spectral region under study) in this case also agreed with the experimental data.

A number of physical reasons that could be responsible for the aforementioned specific features has already been analysed by us in Ref. [5] and rejected. Therefore we analysed at this stage of study the following phenomena that may be responsible for the appearance of specific features in the dependences $\eta(\lambda)$:

(1) The interference of nonlinear responses of the electronic and phonon subsystems of a sample (the excitation of acoustic and thermal gratings). In this case, the relative weights of contributions of different subsystems and their resonant frequencies are bound to be of primary importance from the point of view of the effects (specific features of the nonlinear response) observed in the experiments.

(2) The splitting of the electronic spectrum of a sample into bands of allowed and forbidden states. For transitions between allowed electronic states, inclusion of the selection rules for the principal and orbital quantum numbers into consideration might be important.

(3) The splitting of the bands of allowed electronic states into spin subbands owing to the spin – spin and spin – orbit interactions. The spin selection rules and the energy splitting of spin subbands may be significant from the point of view of the form observed for the dependence $\eta(\lambda)$.

(4) The additional splitting of the spectrum of allowed electronic subbands into two-dimensional subbands owing to the quantum size effect. The effects observed in the experiments could change with changes in sample thickness.

The dependence $\eta(\lambda)$ in the DFPS method is a set of experimental points representing initial points ($\Delta = 0$) of the corresponding family of dependences $\eta(\Delta)$ in the BP method. Therefore, if the central peak of $\eta(\Delta)$ in the BP method is caused by the spectrally independent excitations of acoustic and/or thermal gratings (see Ref. [5]), the dependence $\eta(\lambda)$ obtained in the DFPS method should be smooth and monotonic. Because this is not the case and one can clearly see well-pronounced spectral features in Fig. 1, the appearance of these features, as well as of the central peak in the dependence $\eta(\Delta)$ in the BP method, should be related to the electronic part of the nonlinear response.

When the electronic spectrum is split into bands and subbands of allowed states taking into account the corresponding selection rules for the transitions between them (see below), all the integrals and sums that enter into the expression for the total nonlinear electronic response [5] break up into several 'coherent' (phased) components. The total number of the latter (the total number of terms in the expression for the electronic response) is determined by looking over all possible combinations of different initial and intermediate electronic states. Further interference of these components may lead to the appearance of certain spectral features in the dependences $\eta(\Delta)$ and $\eta(\lambda)$ in the BP and DFPS methods, respectively.

In our numerical calculations, the band structure of Ni was assumed to be given (see Ref. [5]). The position of the Fermi level for each concrete realisation was corrected in such a way that the number of $4s$ (0.54) and $3d$ (9.46) conduction electrons per cell, which corresponds to the scheme [11] for the population of electronic states in Ni, should be retained. For films with thickness $L = 17 - 25$ nm, which were studied in our experiments, there are so many quantum-size subbands that the manifestations of the quantum-size effect have almost no influence on the calculation results (see Ref. [5]). Because of this, all the dependences $\eta(\lambda)$ presented below will correspond to $L = 5$ nm (the splitting of each band into ten quantum-size subbands).

For a pump pulse with energy density ~ 1 mJ cm^{-2}, the evaluation of the change in temperature for the samples under study, taking into account the specific heat of Ni and neglecting the removal of heat into a substrate, gives $\Delta\Theta \sim 3$ K. However, because of a low heat capacity of the electronic subsystem and a finite rate of heat exchange of the latter with the phonon subsystem, the electron temperature Θ_e may be substantially different from the lattice temperature and may reach 1000 K and higher values [12]. Variations of Θ_e in a range of 300 – 1000 K were found to have almost no effect on the type of the calculated dependences $\eta(\lambda)$. The parameter s of the states involved in electronic transitions [5] also has only a weak effect on the form of the curves $\eta(\lambda)$. Therefore all the calculation data presented below (Figs 2 and 3) will correspond to $\Theta_e = 600$ K and $s = 0.01$.

Thus only three factors were used in our calculations as 'free' (fitting) parameters. Because the splitting of spin subbands is determined only in the state of thermodynamic equilibrium and Θ_e may substantially exceed not only the lattice temperature but also the Curie point for Ni ($\Theta_C = 631$ K [13]), we analysed two limiting situations, namely, the case of the 'ferromagnetic phase' in which the spin splitting exactly corresponds to the data of Ref. [14] and the case of the 'paramagnetic phase' in which this splitting is absent. In the paramagnetic phase, the energy of any allowed electronic state was determined as the half sum of the given energies of the electronic states with opposite spin orientations. For electronic transitions from bound to free states (and in the opposite direction), the selection rules for the orbital quantum number that are valid for an isolated atom may be violated. The mixed states may play an important role. That is why we also analysed two similar limiting situations, namely, the case of a total lift of all prohibitions imposed on the change of the orbital quantum number and spin for the electronic transitions and the case where these selection rules were the same as for an isolated atom. In all numerical realisations, the interband-polarisation relaxation time T_2 was varied in the 100 – 300 fs range.

The results of the numerical calculation of the electronic part of the nonlinear response of a Ni film in the paramagnetic and ferromagnetic phases in the DFPS method for $T_2 = 200$ fs are illustrated by curves 1 – 3 in Fig. 1. Although all the calculated dependences $\eta(\lambda)$ presented here are normalised to the maximum value of η and have certain specific spectral features, they give a satisfactory description of the experimental data (the solid curve in Fig. 1) only in the case of the ferromagnetic phase taking into account the spin selection rules (curve 1 in Fig. 1). Moreover, even in this case, variations of T_2 in the 100 – 300 fs range lead to radical changes in the dependence $\eta(\lambda)$ and the relation between the maximum and minimum values of η in the spectral region under study (Fig. 2). In

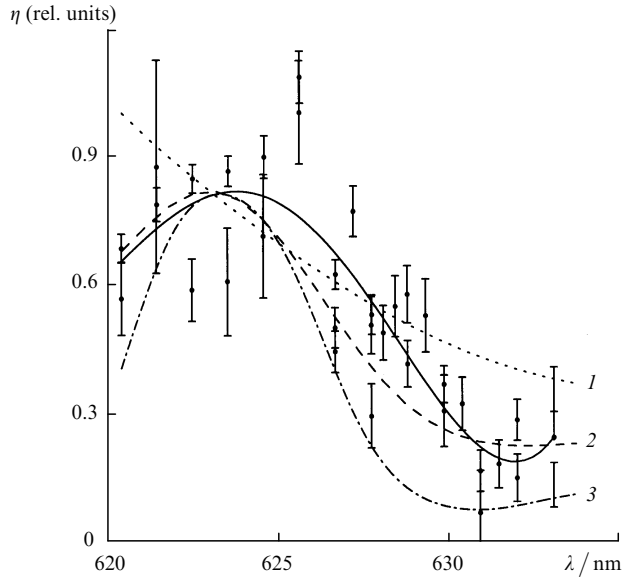

Figure 2. Experimental dependences $\eta(\lambda)$ for Ni (points and solid curve) for $L = 17$ nm and the results of the calculation made for the ferromagnetic phase taking into account the spin selection rules for $T_2 = 100$ (1), 200 (2), and 300 fs (3), $L = 5$ nm, $\Theta_e = 600$ K, and $s = 0.01$.

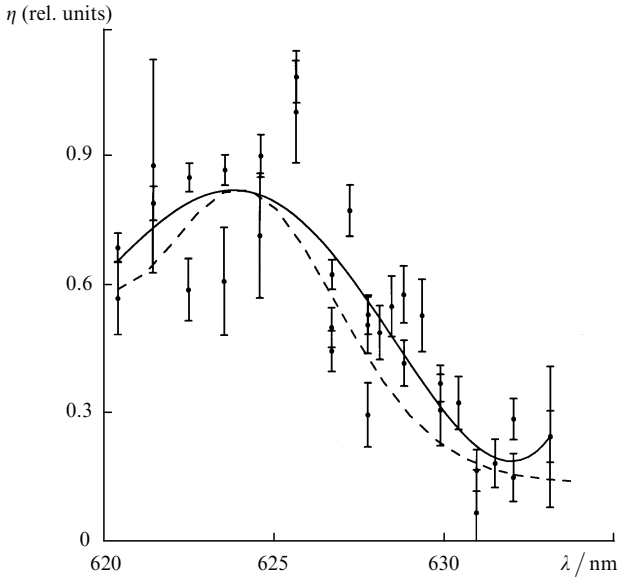

Figure 3. Experimental dependences $\eta(\lambda)$ (points and the solid curve) for the Ni film with $L = 17$ nm and the results of the calculation made for the ferromagnetic phase with a partial (1.5%) lift of spin selection rules for $L = 5$ nm (dashed curve), $\Theta_e = 600$ K, $s = 0.01$, and $T_2 = 200$ fs

particular, for $T_2 = 100$ fs (curve 1 in Fig. 2) almost all specific spectral features of the electronic part of the nonlinear response of Ni would be absent, and for $T_2 = 300$ fs (curve 3 in Fig. 2) the quantity η was bound to vary in the region $\lambda = 620$–634 nm by a factor greater than 10.

Thus we may state with some certainty that the form of the dependence $\eta(\lambda)$ experimentally observed by us in the DFPS method agrees well with the response calculated for the ferromagnetic phase Ni for $T_2 \sim 200$ fs taking into account the spin selection rules. Although the spectral position of the maximum efficiency of the nonlinear process in this case ($\lambda \sim 623$ nm, curve 2 in Fig. 2) is somewhat different from the experimental data ($\lambda \sim 624$ nm, the solid curve in Fig. 2), one can easily eliminate even this weak disagreement by mixing up an additional 'contribution' of the ferromagnetic phase, with lifted spin selection rules, to the total nonlinear response of Ni (curve 2 in Fig. 1). Our calculation showed (Fig. 3) that the spectral positions of all specific features in the experimental (solid curve) and calculated (dashed curve) dependences $\eta(\lambda)$ in the DFPS method almost agreed completely even when the relative contribution of the ferromagnetic phase with lifted spin selection rules was as low as 1.5%.

5. Conclusions

The analysis of the experimental data obtained by the DFPS method suggests that the electronic subsystem makes the dominant contribution to the nonlinear response of the ultrathin Ni films to picosecond laser pulses. It is likely that the characteristic spectral features (the 'peak' of the self-diffraction efficiency η at $\lambda \sim 625$ nm and the 'dip' of η at $\lambda \sim 632$ nm) in the dependence $\eta(\lambda)$ are due to the fact that the Fermi level in the band structure of Ni simultaneously crosses $4s$ and $3p$ subbands.

Thus these specific features are most likely caused by the interference of the contributions of the two aforementioned bands to the total nonlinear response. Although the electronic subsystem of the Ni films under study is heated due to absorption of picosecond laser pulses up to temperatures ~800 K (the subsystem temperature becomes different from the lattice temperature and certainly exceeds the Curie temperature), the spin splitting of the electronic spectrum seems to be retained and the selection rules for the spin and orbital quantum numbers still work. This agrees with the data of Ref. [12], where it was shown that Ni films, heated by a picosecond laser pulse to temperatures exceeding the Curie temperature by almost a factor of two, remained magnetised.

Comparing the results of numerical simulation of the dependence $\eta(\Delta)$ (the BP method) with the experimental data allowed us to obtain only the lower estimate of the interband-polarisation relaxation time $T_2 > 200$ fs (see Ref. [5]). The DFPS method was found to have a considerably higher sensitivity to the change of this parameter, which is the only one free parameter for it. Here, variations of T_2 in a relatively narrow range (100 – 300 fs) cause no changes in the positions of specific features in the calculated dependences $\eta(\lambda)$, but cause radical changes in the dynamic range η in the spectral region under study (see Fig. 2). Because of this, we found from the interpretation of the experimental data obtained by the DFPS method that the ultrathin Ni films under study had $T_2 \sim 200$ fs. Although it was reasonable to expect that the relaxation times in Ni were smaller by an order of magnitude because of a high concentration of free carriers in metals, the estimate agrees with the relaxation times typical of semiconductors [15]. This estimate also agrees with the results of other studies of a number of metals in Refs [1, 2, 9, 12], which, in particular, present the electronic relaxation time of ~500 fs for gold [2].

None of the conclusions presented above contradicts our experimental data obtained by the BP method [5]. However, one can easily see that analysing the experimental data obtained by the DFPS method made it possible to make conclusions that were considerably more concrete than those made in Ref. [5]. Thus this method of coherent four-photon

spectroscopy, which is rather well known, gave considerably more information in the study of ultrathin Ni films.

Acknowledgements. This work was supported by the Russian Foundation for Basic Research (Grants Nos 98-02-17231 and 96-15-96460), the State Scientific and Technical Programs 'Fundamental Metrology' (Project 2.68) and 'Physics of Quantum and Wave Phenomena', 'Fundamental Spectroscopy Division' (Project 08.02.67).

References

1. Fann W S et al. Phys. Rev. B **46** 13592 (1992)
2. Sun C-K et al. Phys. Rev. B **50** 15337 (1994)
3. Kuzik L A et al. Surf. Sci. **361-362** 882 (1996)
4. Tavger B A, Demikhovskiĭ V Ya Usp. Fiz. Nauk **96** 61 (1968) [Sov. Phys.-Usp. **11** 644 (1969)]
5. Petnikova V M, Rudenko K V, Shuvalov V V Kvantovaya Elektron. (Moscow) **28** 69 (1999) [Quantum Electron. **29** 626 (1999)]
6. Akhmanov S A, Koroteev N I Metody Nelineinoi Optiki v Spektroskopii Rasseyaniya Sveta: Aktivnaya Spektroskopiya Kombinatsionnogo Rasseyaniya Sveta (Methods of Nonlinear Optics in the Spectroscopy of Light Scattering: Active Raman Spectroscopy) (Moscow: Nauka, 1981)
7. Kharchenko M A, Petnikova V M, Shuvalov V V Phys. Lett. A **125** 347 (1987)
8. Chekalin S V et al. Phys. Rev. Lett. **67** 3860 (1991)
9. Golovlev V V et al. Pisma Zh. Eksp. Teor. Fiz. **55** 441 (1992) [JETP Lett. **55** 450 (1992)]
10. Farzstdinov V M et al. Phys. Rev. B **56** 4176 (1997)
11. Kittel C Introduction to Solid State Physics (New York: Wiley, 1986)
12. Agranat M B et al. Zh. Eksp Teor. Fiz. **86** 1376 (1984)
13. Kikoin I K (Ed.) Tablitsy Fizicheskikh Velichin (Tables of Physical Quantities) (Moscow: Atomizdat, 1976)
14. Marschall E, Bross H Phys Status Solidi B **90** 241 (1978)
15. Kornienko A G et al. J. Appl. Phys. **80** 2396 (1996)